

Similarity in Perception: A Window to Brain Organization

Zach Solan

School of Physics and Astronomy

Tel Aviv University, Tel Aviv 69978, Israel

solan1@post.tau.ac.il

Eytan Ruppin*

School of Mathematics and School of Medicine

Departments of Computer Science & Physiology

Tel Aviv University, Tel Aviv 69978, Israel

ruppin@math.tau.ac.il

June 6, 1999

Abstract

This paper presents a neural model of similarity perception in identification tasks. It is based on self-organizing maps and population coding and is examined through five different identification experiments. Simulating an identification task, the neural model generates a confusion matrix that can be compared directly with that of human subjects. The model achieves a fairly accurate match with the pertaining experimental data both during training and thereafter. To achieve this fit, we find that the entire activity in the network should decline while learning the identification task, and that the population encoding of the specific stimuli should become sparse as the network organizes. Our results thus suggest that a self-organizing neural model employing population coding can account for identification processing, while suggesting computational constraints on the underlying cortical networks.

* To whom correspondence should be addressed.

INTRODUCTION

Similarity is a basic concept in cognitive psychology which is utilized to explore the principles of perception. Theories about similarity aim at explaining when people identify or judge two different stimuli as related (e.g: Ashby & Perrin, 1988; Ashby & Lee, 1991). Experimentally, similarity between objects is measured using different kinds of stimuli and modalities, via two fundamental methods. The first is the direct method, where subjects are asked to explicitly estimate the level of similarity between two objects. The second method is the indirect one, where subjects are asked to identify various stimuli. This method is motivated by the basic assumption that two similar objects tend to be confused more often. In this paper we focus on modeling similarity experiments performed with the indirect method, which is less dependent on attentional levels. Indirect similarity experiments are also performed in animals, making relevant neurophysiological data readily available.

In a typical indirect similarity experiment, the stimuli are presented to the subject in random order. The subject's task is to identify each stimulus by its serial number, and report it as the *subject response*. In case of error in identification, the experimenter informs the subject about the correct answer. The data thus obtained is typically represented in a two dimensional square *confusion matrix*. A cell in row i and column j of the confusion matrix reports the number of times the subject has erroneously identified stimulus i as stimulus j , and the number of the correct responses is reported on the diagonal. Similarity experiments can be categorized by three major characteristics: the modalities involved, the features that construct the stimuli, and the dimension (the number of features) of the stimuli. The similarity experiments modeled in this paper, a

representative set of similarity experiments with simple stimuli, are classified accordingly in Table 1.

Table 1. The five similarity experiments modeled in this paper, classified by their major characteristics.

Experiment	No of Stimuli	Modality	Features	Dimensions
Shepard 1958	9	Visual	Brightness, Saturation	2
Hodge 1962	8	Auditory	Pitch, Duration, Intensity	3
Kornbrot 1978	6	Auditory	Intensity	1
Nosofsky 1987	12	Visual	Brightness, Saturation	2
Nosofsky 1989	16	Visual	Size, Rotation	2

The theoretical analysis of similarity experiments has been traditionally based on metric models. These models represent stimuli as points in a coordinate space such that the observed similarities between items are related to the metric distances between the respective points. That is, the more similar the stimuli are perceived, the closer their representative points are in space. These multidimensional metric representations can be generated by applying multidimensional scaling (MDS) on the confusion matrix data revealing the perceived stimuli as points in a reduced dimensional space. However, in a typical identification task, not all the entries of the diagonal cells are equal and the confusion matrix is not symmetric. That is, subjects tend to identify some stimuli better than others and stimulus *i* may be more confused with stimulus *j* than vice versa. Thus, the metric representation of stimuli in space has classically been complemented by asymmetric processes involving two main approaches (for more extensive review see Nosofsky, 1992). The first is the *deterministic* approach in which each stimulus (object) is represented as a point in a multidimensional space as in the traditional view, but

employing an additional set of choice decision rules. An important representative of this approach is the *Multidimensional Scaling* (MDS) choice model (Shepard 1957; Luce 1963), which has been able to account for both the asymmetric and the unequal self identification characteristics of the data. According to this model, the probability that stimuli i is identified as stimuli j is an outcome of the choice model decision rule:

$$(1) \quad P(R_j | S_i) = \frac{b_j \eta_{ij}}{\sum_k b_k \eta_{ik}}$$

where η_{ij} is the similarity between stimulus i and stimulus j , a decreasing monotonic function (exponential or Gaussian) of the distance in perceptual space between stimulus i and stimulus j . b_j denotes bias parameters that are associated with each stimulus. The model free parameters are the bias and the location of each stimulus in the multi-dimensions perceptual space. Thus, the amount of free parameters scales linearly with the number of stimuli and dimensions of the perceptual space.

In the second, *probabilistic* approach, each stimulus is represented as a statistical ensemble of points. An important representative of this approach is General Recognition Theory (GRT) (Ashby & Townsend, 1986; Ashby & Perrin, 1988). GRT is based on the assumption that noise is an inherent component in the perceptual system. Hence, across trials, the repeated presentation of the same stimulus gives rise to a probabilistic distribution around the expected values of stimulus representations. In an identification task, GRT assumes the subject divides the perceptual space into regions. In each trial the subject determines within which *decision boundaries* the stimulus representation falls, and this leads to the associated response. GRT accounts for the asymmetric nature of the data by allotting regions of different sizes to the representation of different stimuli. In order to fit the psychological data the model free parameters are the decision boundaries

for each stimulus and its location in the multi-dimensions perceptual space. These approaches provide an excellent fit for the empirical data, but do not account for the representation of similarity in neural terms. Moreover, these approaches embody a very large number of parameters (a few tens) that should be explicitly set to correctly fit the data in a specific manner for each different experiment. As will become evident, the model proposed in this paper points to an interesting connection between the MDS and GRT models of identification.

Several attempts have been previously made to identify the neural correlates of similarity perception in the brain (Edelman, 1995, 1997; Tadashi et al., 1998). A few researchers have performed experiments of odor identification in rats (Youngentob et al., 1990; Kent et al., 1995). They analyzed the perceptual odor stimulus space by applying MDS analysis to a confusion matrix of five different odor stimuli, which resulted in a reduced 2-dimensional space. Examining the neural activity of the olfactory mucosa during odor inhalation, they found that each odorant had a unique "hot spot" region of maximum sensitivity. A y preserving mapping between the position of the corresponding odorant in the reduced 2-dimensional psychophysical odor space and the mucosa location of these "hot spots" was identified. Wang et al. (1996) have investigated the functional organization of object recognition, using optical imaging in inferotemporal cortex, again finding a regional clustering of cells responding to similar features. Young and Yamane (1992) have shown that the encoding of the visual perceptual space of familiar human faces in the inferotemporal cortex of monkeys is population based. This population encoding is sparse and is related to the spatial properties of face stimuli in the corresponding MDS psychophysical space. Put together, these findings support the notion that the processing in some cortical regions engaged in perception employs both a

topological mapping and population coding. A model relating between topological mapping and population coding has been previously suggested by Guenther & Gjaja, (1996) in order to provide an explanation for the well known phenomenon of the *perceptual magnet effect* (Kuhl, 1991). While Guenther & Gjaja's, work models a different set of data, their model of stimulus discriminability has a close relation to similarity perception, inferring perceptual stimulus relations from map activities. Their model, as in our current paper, suggests that the perceptual effects observed in the psychological experiments arise as a natural consequence of the formation and the organization of the neural map.

The observation of Kent et al. (1995) that there is a topological mapping from the perceptual similarity space to its representation in the olfactory mucosa, obviously raises the question of the possible neural mechanisms underlying this phenomenon. A natural candidate is the Self-Organizing Map (SOM) algorithm (Kohonen, 1982), which has been shown (see Kaski 1997 for a review) to be strongly related to the MDS procedure, both maintaining a structural topological mapping. The SOM algorithm, to be described in detail in the next section, has an explicit neural level realization. In this paper, we study a neural model of similarity perception that is based on an SOM topological mapping and population coding. As will be seen, the quest to model the psychophysical data of similarity perception suggests useful constraints on the pertaining neurophysiological level. The next section provides an overview of the model and our simulation experiments. The Results section compares the computational results with the human data. The last section discusses brain organization and development in lieu of our results.

THE MODEL

Model Overview

The model is based on a self-organizing neural network (Kohonen, 1982, 1989) that is implemented in computer simulations. In order to describe the model in a concrete fashion, we refer to a typical indirect similarity experiment performed by Shepard (1958). This well known experiment used 9 stimuli of distinct red colored chips of uniform size. The colored chips, as specified by the system of Munsell, were of a constant hue, but varied in brightness (4 levels) and saturation (4 levels of chroma). Each chip was labeled by a number from “1” to “9”. After a short period of training, 36 subjects were asked to identify the exposed colored chips by their labels. In case of an identification error, the experimenter provided the subject with the correct answer. Each of the 36 subjects was exposed to a random sequence of 200 successive chip identification trials and their responses were assembled in a typical 9X9 confusion matrix (Table 2).

The model is composed of a network of laterally interacting neurons arranged in a two-dimensional array, encoding distinct features of the input stimuli. The neurons are fully connected to a common layer of input neurons as portrayed in Figure 1.

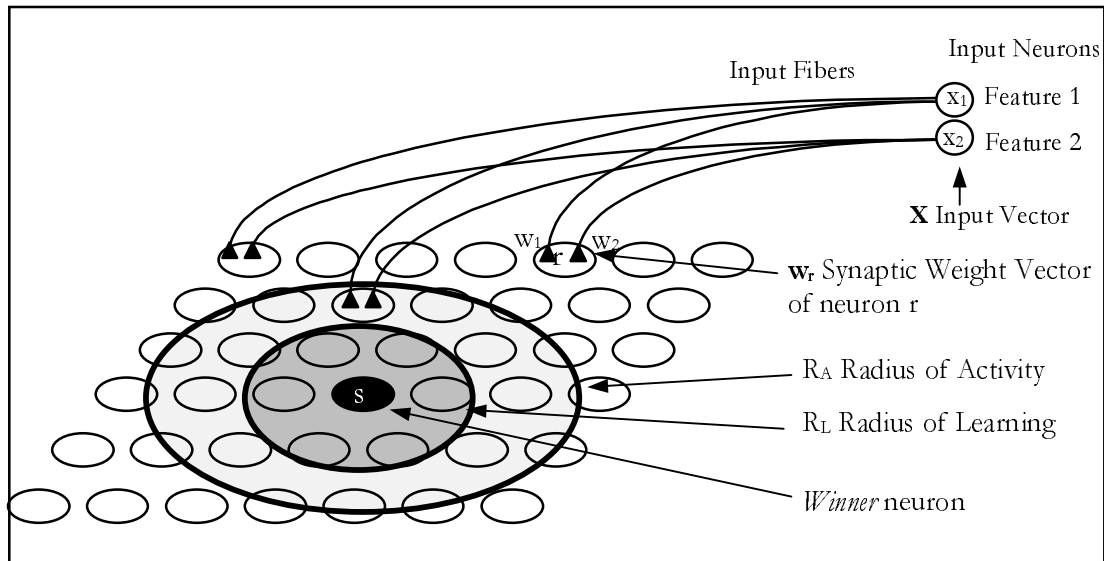


Figure 1. Schematic Model description. The neural model is composed of a two-dimensional array of neurons fully connected to a common source of input fibers transmitting the input stimuli.

To simulate this experiment, the neural network was presented with 2-dimensional input feature vectors representing the 9 stimuli of the original experiment. The value of each of the two components of an input *prototype vector* was determined by the corresponding feature value (i.e., brightness and saturation) of the stimulus it represents. To generate an input vector a random noise term is added to each one of the prototype vector components representing an external noisy environment.

When an input vector is presented and processed by the network, the identification response of the neural model can be “read” from its activity state. The network responses to the representation of a set of stimuli are accumulated in a confusion matrix in a standard manner. The readout of the output data is based on *population coding* (Georgopoulos et al., 1982,1984). In contrast with the *Winner-Take-All* approach, population coding is a method that determines the location of a response vector in the network’s “perceptual” space as a function of the entire network’s activity and not the

result of a single neuron's activity. The model's operation consists of two conceptually distinct phases: The *training phase*, during which the network gradually self-organizes, extracting the regularities of the input stimuli, and the *identification (performance) phase*, during which the organized network can successfully simulate identification tasks. Stimulus identification may also be performed during the training phase, to simulate identification tasks performed early in the learning process.

The Training Phase

In the training phase, the ensemble of input vectors presented to the network is generated according to the following process: A prototype feature vector representing one of the stimuli in the identification experiment is randomly selected. Then, to generate an input vector \mathbf{x} , a noise term is added to each of its n components representing an external noisy environment (typically $n=2$ or 3 , the noise is normally distributed with zero mean, fixed variance and zero covariance). The magnitude of all the input vectors is kept normalized, thus eliminating a scaling bias (see Appendix I for details). The presentation of an input vector gives rise to excitation of neurons in the network array (see Figure 1). The response of neuron r is specified by its n -dimensional synaptic weight vector \mathbf{w}_r and is equal to the dot product of $\mathbf{x} \cdot \mathbf{w}_r$ (Kohonen, 1989, 1993). In response to a given input stimulus, the most active neuron in the lattice (for which $\mathbf{x} \cdot \mathbf{w}_r$ is maximal) is defined as the *winner* neuron, s . Its surrounding network activity is modulated by a Gaussian kernel function $h_{R_A}(\mathbf{r})$ centered on neuron s , whose variance R_A^2 controls the *radius of activation* around the winner ($h_{R_A}(\mathbf{r})$ is largest at $r=s$ and declines monotonically to zero with increasing distance between the s and the r 'th neuron),

$$(2) \ h_{R_A}(r) = \exp\left(-\frac{\|r - s\|^2}{2 \cdot R_A^2}\right).$$

The activity m_r of neuron r is defined as

$$(3) \ m_r = (\mathbf{x} \cdot \mathbf{w}_r) \cdot h_{R_A}(r).$$

During training, the network self-organizes by modifying the synaptic weights of the neurons in the winner's surroundings by

$$(4) \ \mathbf{w}_r^{(new)} = \mathbf{w}_r^{(old)} + \varepsilon \cdot h_{R_L}(r) \cdot (\mathbf{x} - \mathbf{w}_r^{(old)})$$

$$(5) \ h_{R_L}(r) = \exp\left(-\frac{\|r - s\|^2}{2 \cdot R_L^2}\right),$$

where $h_{R_L}(r)$ is a Gaussian function whose variance R_L^2 (*radius of learning*) controls the region of synaptic modification around the winner, and ε is a *learning rate* that governs the rate of synaptic modification.

For the map to converge, R_L and ε must decrease over time (in our simulations they are decreased in a linear rate). The first, rapid, stage of map organization is conventionally termed *spread out*, and is characterized by global synaptic changes. The second, *fine tuning* phase, occurs after the topological ordering of the map is established and is characterized by slow local synaptic changes that permit the convergence of the network's synaptic matrix .

The Identification Phase

In a simulated identification task, the network is exposed to input stimuli vectors generated as in training phase. The synaptic matrix generated previously during the training phase is kept fixed during this phase. The output of the network given an input vector is determined via the *population coding* method (Georgopoulos et al., 1982,1984), i.e, by the vectorial sum of the neurons' synaptic efficacies weighted by their activity

$$(6) \mathbf{p} = \frac{\sum_{r=1}^N m_r \cdot \mathbf{w}_r}{\sum_{r=1}^N m_r},$$

where N is the total number of neurons in the network array, w_r is the synaptic weight vector of neuron r and m_r is its activity. The vectorial sum is made on the entire network and thus, the population vector is an average outcome of the network's activity response to the input stimulus and its reading induces a transformation of the input vectors to a new location in feature space. The final output vector is determined by adding a normal distribution noise term to this new location, simulating an internal noise factor in human processing (the noise levels, both internal and external, are fixed parameters and do not vary in time, Figure 2a). The model's identification response is determined by finding the *prototype population vector*¹ closest to the output vector (i.e., in which decision boundaries it falls in the network's perceptual map, Figure 2b, see also Appendix II). The identification responses over many input stimuli are then summed up in a confusion matrix in a standard manner.

¹ A prototype population vector is a prototype vector that has been transformed using a population coding method.

To simulate the known phenomena that humans tend to guess answers at the initial stages of learning to perform similarity psychology tasks (Shepard, 1958), a “guessing” parameter is introduced. This parameter, following Nosofsky’s model (1987) introduces a random selection of the network response at some small fraction of the learning trials. At the early stages of learning the probability for the network to guess a response is 13.5%, decreasing monotonically as the network learns to 0.5% at the end of the training phase, as in Nosofsky (1987). These dynamics governing the “guessing” parameter are kept fixed throughout our simulations.

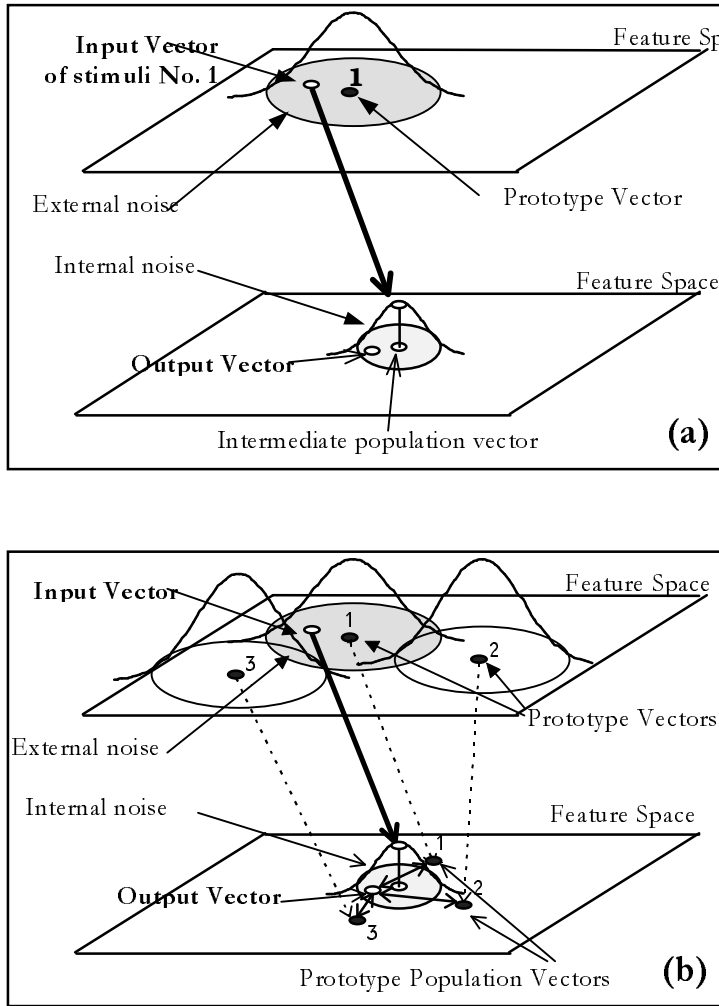


Figure 2. Reading the network’s output. The figure demonstrates the identification process (a) An input vector is chosen from a normal distribution (simulating external noise) centered around a prototype feature vector stimulus (e.g., stimulus No. 1). The network processing assigns an intermediate population vector to the input vector in the feature space. The final output vector is determined by adding a normal distribution noise term to the population vector, simulating internal noise factors in human processing. (b) The output response is then identified by finding which of the prototype population vectors is the closest to the output vector, in the new mapping.

RESULTS

This section reports the model performance on four different identification tasks. We begin by analyzing the identification results of mature fully-trained networks, comparing between the confusion matrices generated by the model and the corresponding confusion matrices of human subjects. Next, we turn back to study the training phase in depth, by

investigating the performance of the model as it evolves and self-organizes while training on the dynamic Munsell's 12 color experiment (Nosofsky, 1987).

Identification

The first experiment analyzed is the similarity experiment of Shepard (1958, see previous section 2.1) which used 9 different Munsell's red colored chips with constant hue, varying in brightness and saturation. The network lattice had 1200 neurons (40X30) fully connected to two input feature neurons coding the stimuli's brightness and saturation. The input vectors were generated from 9 two-dimensional feature vectors of the original stimuli employed in the task, with additional normal distributions of external ($\langle\sigma\rangle=1.06$) and internal noise ($\langle\sigma\rangle=0.05$). Table 2 presents a comparison between the experimentally observed confusion matrix (human performance, top dark line in each row) and the confusion matrix generated by the model (second line).

All the results presented henceforth were obtained by averaging the identification performance of 100 networks employing identical dynamical parameters, but varying the initial values of the network's synaptic weights, simulating a population of 100 "subjects".

Table 2. Comparison between the *observed* and *predicted* confusion matrices of Shepard's (1958) task. In each row of the matrix, the top dark line indicates the observed frequencies from the experimental data, the second line indicates the frequencies generated by the model and the third line depicts their *standard error*. All values are rounded to the closest integer.

	1	2	3	4	5	6	7	8	9
1	136	30	11	6	5	4	3	2	3
	145	35	2	12	2	1	2	0	1
	(16)	(11)	(4)	(10)	(2)	(1)	(1)	(5)	(1)
2	33	109	13	15	11	3	9	4	3
	24	119	7	21	17	2	6	2	1
	(10)	(15)	(6)	(13)	(10)	(2)	(2)	(6)	(2)
3	12	14	123	3	21	13	4	6	3
	1	9	125	2	22	30	1	9	1
	(3)	(7)	(18)	(3)	(18)	(17)	(17)	(2)	(9)
4	3	21	3	108	11	1	33	6	13
	10	21	1	123	9	1	25	1	9
	(8)	(11)	(1)	(19)	(8)	(1)	(1)	(18)	(2)
5	7	14	24	11	92	15	11	20	6
	2	18	18	11	110	8	17	16	2
	(2)	(8)	(10)	(9)	(17)	(7)	(7)	(9)	(12)
6	5	6	11	3	7	143	3	19	3
	0	1	29	1	7	128	1	31	1
	(1)	(2)	(16)	(1)	(7)	(18)	(18)	(2)	(17)
7	2	7	3	29	10	3	107	10	29
	2	6	2	26	14	2	119	7	23
	(4)	(4)	(2)	(17)	(10)	(2)	(2)	(17)	(6)
8	3	5	6	9	14	19	11	126	7
	0	2	9	2	19	33	9	124	2
	(1)	(2)	(9)	(2)	(15)	(18)	(8)	(19)	(2)
9	1	3	2	14	4	4	12	4	156
	1	2	0	13	2	1	32	1	148
	(2)	(2)	(1)	(12)	(3)	(1)	(15)	(1)	(18)

Three major indices have been calculated to examine the quality of fit between the experimentally observed and model predicted matrices: the *Correlation*, the *Sum-Squares Error* and the *Likelihood Ratio*.

The correlation between the matrices is a somewhat problematic index, since the largest values are concentrated on the diagonal. The correlation index, which gives higher weight to the similarity between high-valued cells, may thus give high correlation values for matrices with similar diagonals, but that still may significantly differ on their off-diagonal terms. Hence, correlation calculations were applied separately to the

diagonal and off-diagonal regions, yielding a diagonal correlation of the data displayed in Table 2 of $r=0.89$ ($t=5.16$, $p<0.005$) (Figure 3) and an off-diagonal correlation of $r=0.80$ ($t=11.15$, $p<0.0005$).

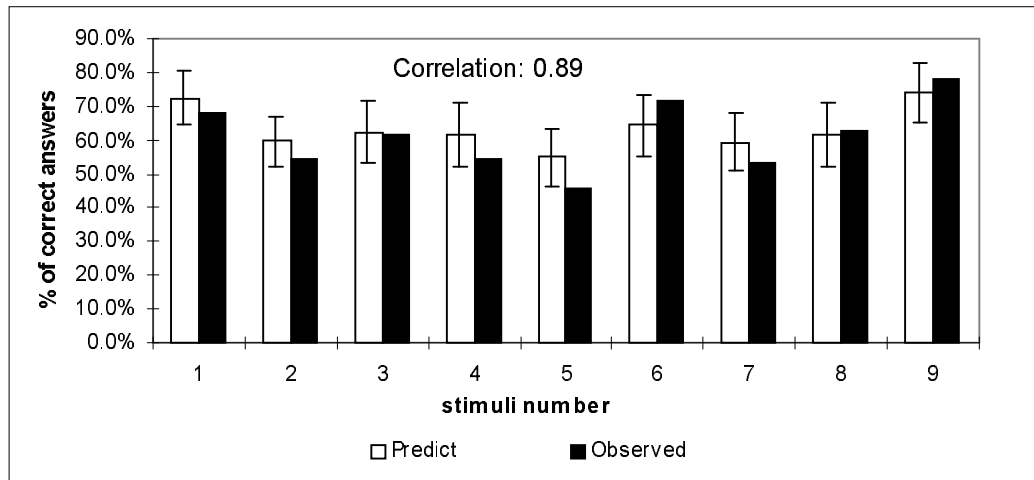


Figure 3. Comparison of predicted versus observed correct identification frequencies (diagonal values) for all 9 stimuli in the Shepard's identification task. Black bars represent the percentage of correct answers in human data, and white bars represent the model generated responses. The standard error of the model responses is portrayed by the error bar on top of the model white bars.

We have also calculated the Sum-Squared Error between the observed and predicted confusion data on the entire matrix (SSE) and on the diagonal alone (DSSE). In order to compare between different experiments, these SSE and DSSE values were normalized by the total number of trials of the experiment. The last index calculated was the log-likelihood ratio testing. This index is often used in similarity experiments to determine the quality of fit, and is utilized to compare the model's performance with those psychological experiments that use this index (See Appendix II).

The pattern of error distribution between predicted and observed frequencies across all matrix entries has a zero mean, testifying to the absence of a systematic bias (drift) in the predicted confusion matrix.

In addition to Shepard's experiments, similar simulation experiments and analysis were performed to simulate four other identification tasks. The results, summarized in Table 3, testify to the ability of the network model to provide a close fit to a wide variety of pertaining experimental data. Yet, the model results are not as good as those achieved previously with the best MDS choice models. The latter embody a much larger number of free parameters to fit the data and perhaps more important, their kernel functions are varied across experiments.

Table 3. An overview of the results of simulating five different similarity experiments. The model's results are compared with their strongest adversary, i.e., with the best fit achieved in each experiment.

Experiment	No. of Subjects	No. of Stimuli	Dim	Model	Correlation			Sum Square Error		
					Free Parameters	Diagonal	Non diagonal	Total	Diagonal (DSSE)	Total (SSE)
Shepard 1958	36	9	2	Neural	2	0.89	0.80	0.98	0.6±0.4	2.1±0.9
				MDS-Choice	28	0.99	0.95	0.99	0.15	0.43
Hodge 1962 ²	6	8	3	Neural	2	0.87	0.75	0.97	2.7±0.8	4.5±1.0
Kornbrot 1978 ³ Subject 1	1	8	1	Neural	2	0.87	0.97	0.97	0.3±0.4	2.4±0.7
				Gaussian MDS-Choice	14	0.99	0.99	0.99	0.22	0.61
Subject 2	1	8	1	Neural	2	0.85	0.87	0.93	1.5±0.8	3.3±1.0
				Gaussian MDS-Choice	14	0.97	0.99	0.99	0.22	0.61
Nosofsky 1989	57	16	2	Neural	2	0.80	0.88	0.94	0.8±0.2	4.2±0.4
				Gaussian MDS-Choice	45	0.98	0.97	0.99	0.23	1.02

² Hodge and Pollack's (1962) experimental data appear in Nakatani 1972.

³ Kornbrot's (1978) experimental data is reexamined in Nosofsky 1985.

Learning Identification

Next we provide a detailed description of the way the model develops and self-organizes through training on the dynamic Munsell's 12 colors experiment (Nosofsky, 1987). The experiment of Nosofsky is especially interesting since it provides a unique sequence of three consecutive confusion matrices, which are obtained from human subjects as they learn the task. This data provides strong experimented constraints on the self-organization process of the simulated map representation. In Nosofsky's experiment the stimuli were 12 Munsell colored chips with constant red hue (5R). The colored chips were varied in brightness and saturation. Nosofsky's experimental session was organized in 3 blocks of 108 trials each, and a confusion matrix was obtained for each block. *Block 1* denotes the confusion matrix obtained after the first 108 trials, *Block 2* after 216 trials and *Block 3* after 324 trials. As in the previous simulation of Shepard's experiment, the input stimuli were generated from 12 2-dimensional feature vectors of the original stimuli with normal distribution of external noise ($\langle\sigma\rangle=1.06$) and internal noise ($\langle\sigma\rangle=0.05$), in a network array of 1200 neurons (40X30). While training the network by repeatedly presenting input vectors from this distribution and applying the dynamics defined in Equation (4), the learning radius R_L was gradually reduced from $R_L=15$ to $R_L=1$ in a total of 25,000 iterations. In each of these decreasing R_L steps, 30 different radius of activity levels were applied ($R_A=30..1$) and a confusion matrix was obtained for each (R_L, R_A) pair. Hence, in total, the model has provided 450 (15X30) confusion matrices, each with a different R_A - R_L combination⁴. (As describe in the Model section, the two free

⁴ Note that this procedure is made possible since R_A does not take part in the network self-organization dynamics during training, and therefore the same network (i.e., with a given R_L value) can be used to generate different confusion matrices by varying the value of R_A without affecting its self-organization.

parameters R_L and R_A represent the radius of synaptic changes around the winner neuron and its neighborhood activity, respectively).

In order to study the capability of the network to simulate the dynamics of learning, i.e., to fit all three experimental confusion matrices gradually as the network self-organizes and develops, we compared each one of the 450 simulation-generated matrices with each of the three experimental human block matrices, using the normalized DSSE index. Figure 4 describes the resulting DSSE index for three levels of learning radius R_L ($R_L = 10, 7, 4$), varying the activity radius R_A . For a given R_L level, each figure contains three curves, depicting the accuracy by which the model's results match the experimental data contained in Nosofsky's three learning blocks, as a function of R_A . For a given block the best fit is achieved when its corresponding curve gets its minimum error value. The Figure emphasizes the fact that the ability of the neural model to predict the three blocks is highly influenced by the values of R_L and R_A .

At the very beginning of the learning, immediately after the *spread out* phase, ($R_L = 10$ fig 4a), Block 1 achieves the maximal fit with the model's generated confusion matrices for all possible R_A levels. Later, when $R_L = 7$ (fig 4b), block 2 already succeeds in replacing block 1 as the best fit at lower R_A values ($R_A < 17$). Through training as R_L decreases (this is necessary otherwise the map will not converge and stabilize), there is a critical R_L level below which the model can successfully fit all three experimental blocks. The best fit of the model's confusion matrix transitions as R_A is decreased from Block 1 to Block 2 to Block 3 ($R_L = 4$, fig 4c), precisely in the same order of their occurrence in the human psychological experiments. Hence, we find that *in order to fit the psychological data, R_A must decrease with learning*. The activity in the entire network must hence decrease as the network learns (see Figure 5a). Nosofsky's (1987) experiment

is similar to that performed by Shepard (1958), where the confusion matrix was obtained after 200 trials. Remarkably, the R_A - R_L values providing the best fit with the experimental data of Shepard fit well with best fit R_A - R_L plot found for Nosofsky's data, as shown in Figure 5b.

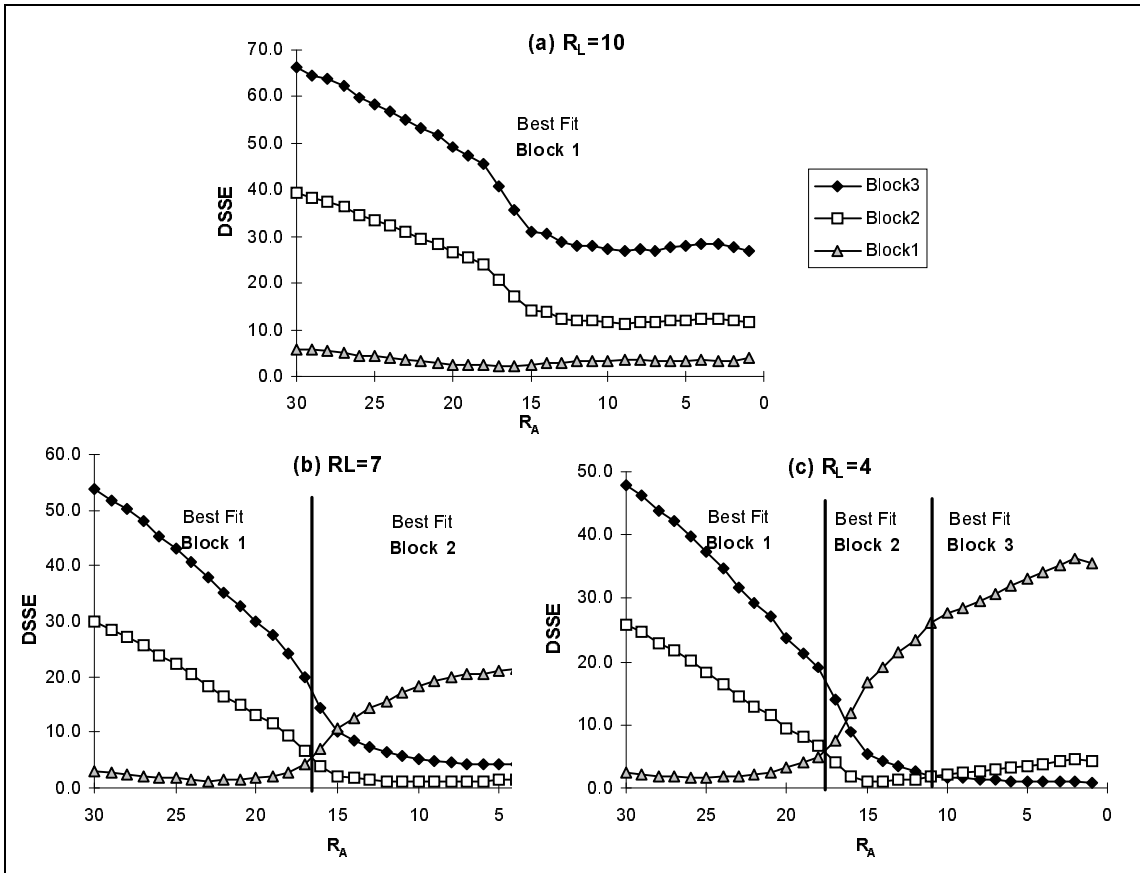


Figure 4. The normalized DSSE (Diagonal Sum Square Error) when modeling Nosofsky's data (1987). The three plots describe the value of the normalized DSSE index (y-axis) as the function of R_A (x-axis), for different R_L values. The gray triangles represent the fit with Block 1, the white rectangles represent the fit with Block 2 and the black diamonds represent the fit with Block 3.

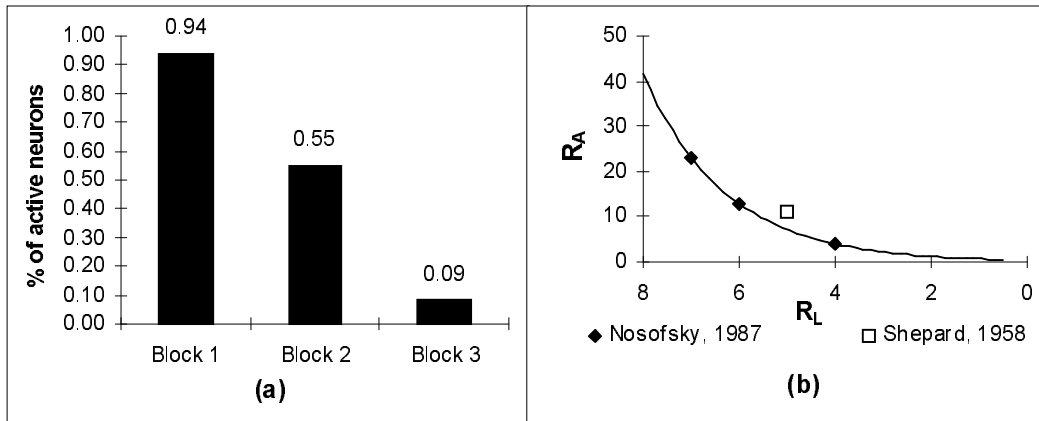


Figure 5. (a) Network activity during learning. The x-axis is the percentage of active neurons in the network. A neuron is considered "active" when its activity passes a threshold value of 20% of the *winner's* activity. The activity in the best fit networks decreases during training. (b) The best fit combination of R_A versus R_L . The black diamonds represent the best fit combinations for the Nosofsky (1987) experiment. The white square represents the best fit R_A - R_L combination for Shepard's (1958) experiment.

Table 4 summarizes the simulation performance of the model in Nosofsky's experiment and compares it with two kinds of models. One is the classical multi-parametric MDS choice model and the second is a version of the dynamic choice model simulated by Nosofsky (1987). To reduce the number of parameters used, the simulation version of the choice model performed by Nosofsky used the original feature coordinates in order to fit the data with a bias free dynamic choice model. As evident in Table 4, the neural model and the simulated dynamic choice model achieve similar levels of fit as measured by the log-likelihood index.

Table 4. Performance during training on Nosofsky's dynamic 12 Munsell's color experiment.

Experiment	Model	Correlation			Sum Square Error		Log-Likelihood Ratio	
		Free Parameters	Non diagonal	Total	Diagonal (DSSE)	Total (SSE)		
Nosofsky 1987								
Block 1	Neural	2	0.78	0.74	0.95	1.4±0.5	4.7±0.8	-585±75
	MDS	35	0.95	0.93	0.99	0.3	1.3	-386
	Dynamic Choice							
	Simulation of Dynamic Choice	2						-532
Block 2	Neural	2	0.86	0.72	0.98	0.9±0.4	4.2±0.7	-528±28
	MDS	35	0.97	0.98	0.99	0.2	0.6	-268
	Choice							
	Simulation of Dynamic Choice	2						-505
Block 3	Neural	2	0.83	0.77	0.99	0.9±0.3	2.5±0.4	-395±19
	MDS	35	0.97	0.95	0.99	0.2	0.5	-235
	Choice							
	Simulation of Dynamic Choice	2						-403

Understanding the model's operation requires an investigation of the effect of training on the network's feature space. Figure 6 displays the spatial organization of the prototype population vectors in the three network training states leading to maximal fit with Blocks 1, 2 and 3 respectively. The results demonstrate that representation of stimuli becomes more discriminable over time, as the distances between the prototype population vectors increases. Thus, the effect of the internal noise decreases (even though its absolute magnitude remains fixed) and the identification performance gradually improves.

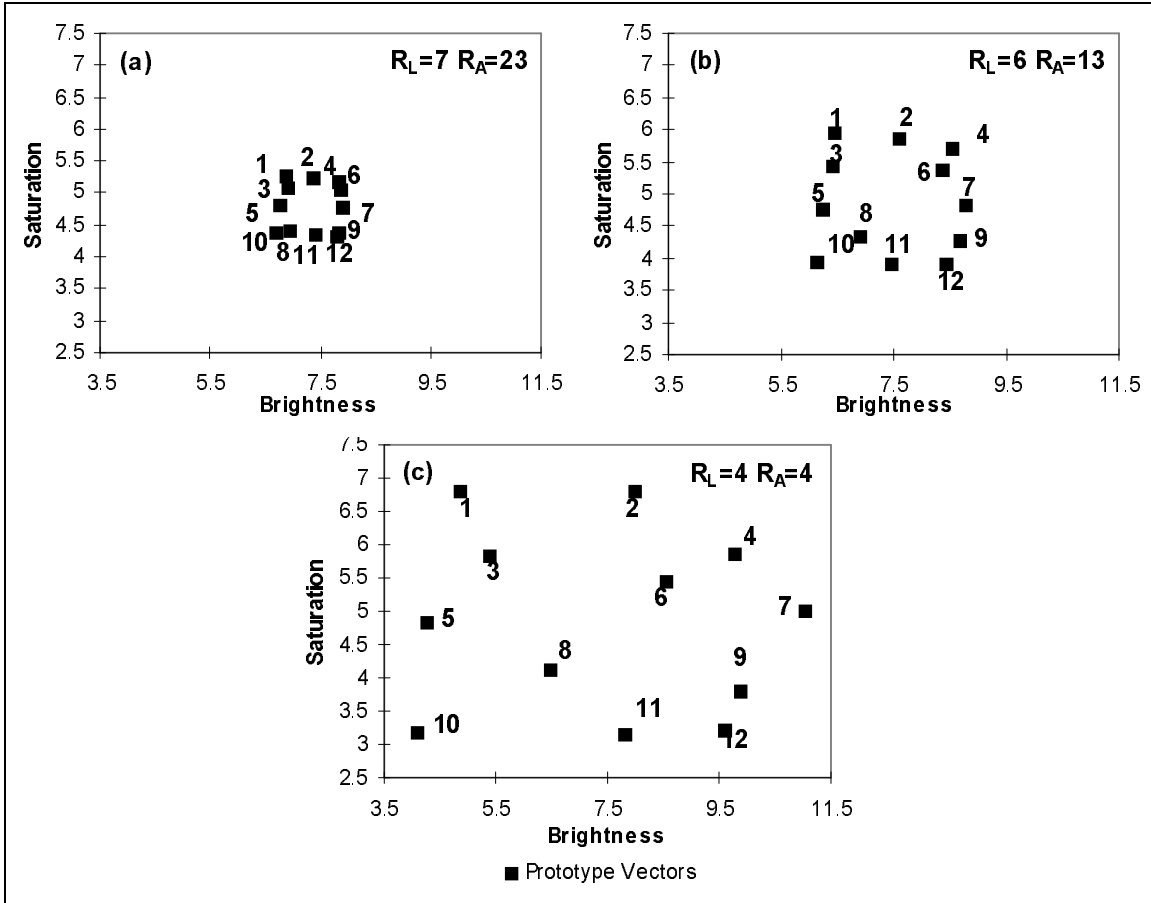


Figure 6. Spatial organization of the prototype population vectors during training. The figure depicts the population encoding representations of the prototype vectors in the brightness/ saturation feature space (solid squares). Time (training) progresses from subfigure (a) to (c).

Imposing Winner-Take-All (WTA) constraints on R_A (by keeping R_A constant and equal to 1 through training) results in a severe degradation in the ability of the model to fit the data (Figure 7). The WTA approach provides a good fit only towards the end of training while at earlier stages its DSSE and SSE error indices are more than twice than those achieved while optimally decreasing R_A as a function of R_L ⁵.

⁵ It should be noted that R_L and R_A are not symmetric in the sense that R_L is a crucial parameter for network convergence and thus must gradually decrease over time. R_A , in contrast, is significant only for

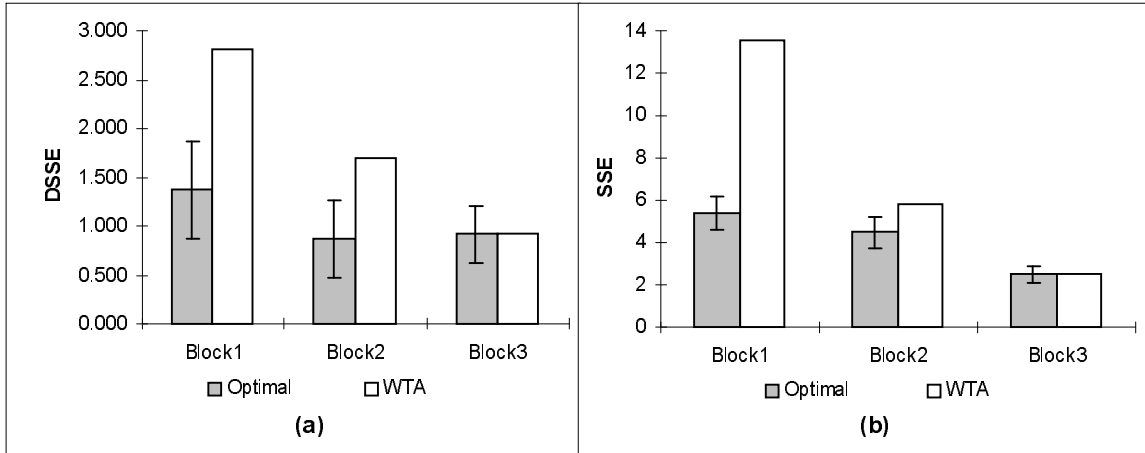


Figure 7. Quality of fit with fixed $R_A=1$ (WTA constraint) versus optimal R_A variation and population coding simulating Nosofsky's experiment. The optimal R_A variation and population coding is represented by the gray bar, the WTA constraint is represented by a white bar. (a) The DSSE index (y-axis). (b) The SSE index (y-axis). The standard error of the optimal R_A-R_L variation is portrayed by the error bar on top of the gray bars.

DISCUSSION

In this study we have explored the ability of a neural model of similarity perception to simulate five different indirect similarity experiments. Identifying a set of input stimuli feature vectors, the model generates a confusion matrix that can be compared directly with the pertaining experimental data. Our results suggest that self-organizing maps based on the dynamics of population coding can model human responses fairly accurately, using very few parameters. The principal findings suggest that in order to obtain a good fit with the psychological data, the activity in the entire network must

"reading" the network's identification output, and its variation does not affect the organization of neural map.

gradually decrease while learning the task. Thus, the model predicts that simultaneously with a gradual reduction in synaptic modifications, the network activity should also gradually decline. To obtain a good fit one must use a population coding approach instead of the perhaps more conventional WTA method for “reading” the network’s output. Finally, the model produces a reasonable fit to the experimental data of 3-dimensional perceptual space (Hodge 1962, See Table 3), where the SOM mapping to the 2 dimensional network array also involves a reduction in the number of dimensions.

The topological organization and population coding characteristics of the neural model find support in animal experiments of similarity as briefly reviewed in the Introduction. Similar evidence for topographical maps has been recently found also in higher perceptual levels (Fujita et al, 1992; Gochin et al, 1991; Wang et al., 1996; Tanaka, 1996). The sparse population coding found in identification tasks involving a long training period (e.g., Young & Yamane, 1992) fits with model’s prediction that the activity should drop down as the map organizes.

The neural model presented here shares common fundamental properties with previous psychological models. Like the GRT model, the neural model generates a new representation of the stimuli in the perceptual space. As in GRT, the identification of an input stimulus depends on the boundaries in which the stimulus’ representation falls in. The asymmetric relations are due to the asymmetric amounts of overlap between the distributions corresponding to each class.. However, the GRT model relies on an explicit ongoing supervised comparison between the stimuli and their representations in the model to further adjust the model parameters to obtain maximal fit. In contrast, the neural model achieves this maximization goal in a self-organizing unsupervised manner. This property places our model in an ideal position to provide a natural, on line, account

of identification during training in neural terms. The neural model also shares common computational principles with the MDS approach, since the topologically preserving algorithm of the SOM well approximates the operation of a metric preserving algorithm like MDS (Kaski, 1997). However, an important distinction between the operation of our model and MDS-based choice models is that the output identification in the neural model is performed in the original (possibly high-dimensional) feature space and not in the reduced MDS space. In summary, the SOM-related neural model proposed here provides an interesting example for a possible identification mechanism which incorporates both GRT and MDS-like dynamics, suggesting that in some sense both these approaches may play a part in similarity identification in the brain.

The main advantage of our model over previous MDS-choice and GRT models is that it provides a neural level description for similarity perception in the brain. While some of the earlier psychological mathematical models have obtained better fit with the experimental data, the neural model obtains a fairly close fits to the data considering the very few free parameters it uses. *Furthermore, it should be emphasized that the number of parameters embodied by the neural model is independent of the dimension and number of stimuli.* The model uses only two free parameters (R_L , R_A), given fixed values of external and internal noise and guessing response, while previous psychological mathematical models have required many free parameters since they rely on an explicit representation of the distances between the stimuli and their biases. The neural model's parameters have a clear meaning in neural terms that helps us to better understand the underlying physiological mechanisms. Since the model dynamics take place in a self-organizing manner, stimulus identification is performed without the need to

explicitly specify many parameters. Instead, the “distances” between stimuli are implicitly defined by the geometry of the self-organized output feature space.

The biological plausibility of the population coding method and the Self-Organizing Map algorithm has been argued by Georgopoulos et al. (1982, 1984) and Kohonen (1993), respectively. The population coding method has been found to provide a fair account of neural activity pattern, during variety tasks and different modalities (e.g., Georgopoulos et al., 1989, Schwartz, 1994). The Winner-Take-All function can be implemented by laterally connected network with excitatory short range lateral feedback connections and inhibitory longer range ones. Under these conditions a “peak” of activity is formed at the neural cluster that best matches the external input. The learning procedure can be implemented by synaptic interactions that are mediated via a diffuse chemical agent (grossly represented in our model by the R_L parameter). During learning the effective range of the diffuse chemical modulation is decreased from a fairly wide to a narrow value. A good candidate for the diffuse neuromodulator agent may be Nitric Oxide (NO) that has been found to be produced in proportion to the postsynaptic potential and to control synaptic plasticity (Fazeli, 1992). The neighborhood activity around the winner neuron can be controlled by an inhibitory process which is represented by the R_A parameter and mainly reflects the activation of the long range inhibitory connections. The realization of such a decrease in the radius of activation surrounding winning neurons may occur in biological networks via the action of second order processes such as neural fatigue and adaptation. The main motivation for assigning distinct parameters for R_L and R_A was that synaptic modifications and neural activity might be governed by different modulation processes such as distinct neuromodulators

and diffuse chemicals. Nevertheless, the finding that these two processes covary in the same direction supports the possibility that one can obtain successful SOM models of similarity perception using activity-dependent Hebbian learning without the need to specify an explicit radius of learning.

In summary, this paper presents a novel neural model of identification, forming a tentative conceptual bridge between the pertaining psychological and neurophysiological data. The need to fit the cognitive experimental data, in turn, suggests interesting constraints concerning brain organization and development in perceptual processing regions.

Acknowledgments

We thank Daniel Algom for his helpful comments and suggestions. Reprints requests should be sent to Eytan Ruppin Departments of Computer Science & Physiology, Tel-Aviv University, Tel-Aviv 69978, Israel, or via e-mail: ruppin@math.tau.ac.il.

References

- Ashby, F. G., & Perrin, N. A. (1988). Toward a unified theory of similarity and recognition. *Psychological Review*, 95, 124-150.
- Ashby, F. G., & Townsend, J. T. (1986). Varieties of perceptual independence. *Psychological Review*, 93, 154-179.
- Ashby, F. G., & Lee, W. W. (1991). Predicting similarity and categorization from identification. *Journal of Experimental Psychology: General*, 120, 150-172.

- Edelman, S. (1995). Representation of similarity in 3D object discrimination. *Neural Computation*, 7, 407-422.
- Edelman, S., & Duvdevani-Bar, S. (1997). Similarity, connectionism and the problem of representation in vision. *Neural Computation*, 9, 701-720.
- Fujita, I., Tanaka, K., Ito, M., & Cheng, K. (1992). Columns for visual features of objects in monkey inferotemporal cortex. *Nature*, 360, 343-346.
- Georgopoulos, A. P., Kalaska, J. F., Caminiti, R., & Massey, J. T. (1982). On the relations between the direction of two-dimensional arm movements and cell discharge in primate motor cortex. *Journal of Neuroscience*, 2, 1527-1537.
- Georgopoulos, A. P., Kalaska, J. F., Crutcher, M. D., Caminiti, R., & Massey, J. T. (1984). The representation of movement direction in the motor cortex: Single cell and population studies. In Edelman, G. M., Gall, W. E, & Cowan, W. M, (Eds.). *Dynamic aspects of neocortex*.
- Georgopoulos, A. P., Lurito, J. T., Petrides, M., Schwartz, A. B., and Massey, J. T. (1989). Mental rotation of the neural population vector. *Science*, 243, 234-236.
- Gochin, P. M., Miller, E. K., Gross, C. G., & Gerstein, G.L. (1991). Functional interactions among neurons in inferior temporal cortex of the awake macaque. *Experimental Brain Research*. 84, 505-516.
- Grajski, K., & Merzenich, M. (1990). Hebb-type dynamics is sufficient to account for the inverse magnification rule in cortical somatotopy. *Neural Computation*. 2, 71-84.
- Guenther F. H., & Gjaja M. N. (1996). The perceptual magnet effect as an emergent property of neural map formation. *Journal of the Acoustical Society of America*, 100, 1111-1130.

- Hodge, M. H. (1962). Confusion matrix analysis of single and multidimensional auditory displays. *Journal of Experimental Psychology*, 63, 129-142.
- Kaski, S. (1997). Data Exploration using self-organizing maps. *Mathematics and Management in Engineering* No. 82, Acta Polytechnica Scandinavica, Finnish Academy of Technology.
- Kent, F. K., Youngentob, S. L., & Paul R. S. (1995). Odorant-specific spatial patterns in mucosal activity predict perceptual differences among odorants. *Journal of Neurophysiology*, 74, 1777-1781.
- Kohonen, T. (1982). Self-organized formation of topologically correct feature maps. *Biological Cybernetics*, 43, 59-69.
- Kohonen, T. (1989). *Self-Organizing and Associative Memory*. (3rd ed.) Springer, Berlin.
- Kohonen, T. (1993). Physiological interpretation of the self-organizing map algorithm. *Neural Networks*, 6, 895-905.
- Kornbrot, D. E. (1978). Theoretical and empirical comparison of Luce's choice model and logistic Thurstone model of categorical judgment. *Perception & Psychophysics*, 24, 193-208.
- Kuhl, P.K. (1991). Human adults and human infants show a 'perceptual magnet effect' for the prototypes of speech categories, monkeys do not. *Perception & Psychophysics*, 50, 93-107.
- Luce, R. D. (1963). Detection and recognition. In *Handbook of mathematical psychology*, Luce, R. D., Bush, R.R., Galanter, E. (Eds.). 1, 103-190. New York: Wiley.

- Nakatani, L.H. (1972). Confusion-choice model for multidimensional psychophysics. *Journal of Mathematical Psychology*, 9, 104-127.
- Nosofsky, R. M. (1985). Luce's choice model and Thurstone's categorical judgment model compared: Kornbrot's data revisited. *Perception & Psychophysics*, 37, 89-91.
- Nosofsky, R.M. (1987). Attention and learning processes in the identification and categorization of integral stimuli. *Journal of Experimental Psychology: Learning Memory & Cognition*, 13, 87-109.
- Nosofsky, R. M. (1989). Further tests of an exemplar-similarity approach to relating identification and categorization. *Perception & Psychophysics*, 45, 279-290.
- Nosofsky, R. M. (1992). Similarity Scaling And Cognitive Process Models. *Annual Review of Psychology*, 43, 25-53.
- Schwartz, A. B. (1994). Direct cortical representation of drawing. *Science*, 265, pp. 540-542.
- Shepard, R. N. (1957). Stimulus and response generalization: A stochastic model relating generalization to distance in psychological space. *Psychometrika*, 22, 325-345.
- Shepard, R.N. (1958). Stimulus and response generalization: Tests of a model relating generalization to distance in psychological space. *Journal of Experimental Psychology*, 55, 509-523.
- Tadashi, S., Edelman, S., & Tanaka, K. (1998). Representation of objective similarity among three-dimensional shapes in the monkey. *Biological Cybernetics*, 78, 1-7.
- Tanaka, K. (1996). Inferotemporal cortex and object vision. *Annual Review of Neuroscience*, 19,109-139.
- Wang, G., Tanaka, K., & Tanifuji, M. (1996). Optical imaging of functional organization in the monkey inferotemporal cortex. *Science*, 272, 1665-1668.

Wickens, T.D. (1982). *Models for behavior: Stochastic processes in psychology*. San Francisco: Freeman.

Young M. P., & Yamane S. (1992). Sparse population coding of faces in the inferotemporal cortex. *Science*, 256, 1327-1331.

Youngentob, S.L., Markert, L.M., Mozell, M.M., & Hornung, D.E. (1990). A method for establishing a five odorant identification confusion matrix task in rats. *Physiology & Behavior*, 47, 1053-1059.

Appendix I - Normalization of input feature stimuli vectors.

In order to normalize the input feature vectors, an agonist-antagonist method was used in the simulations (Guenther & Gjaja, 1996). This method replaces each feature input component x_i with a new agonist-antagonist input of the form

$$(1) \quad x_i^+ = \frac{x_i - x_{iMIN}}{\sqrt{(x_i - x_{iMIN})^2 + (x_{iMAX} - x_i)^2}}$$

$$(2) \quad x_i^- = \frac{x_{iMAX} - x_i}{\sqrt{(x_i - x_{iMIN})^2 + (x_{iMAX} - x_i)^2}}$$

where the index i indicates the feature dimension number, x_i is the value of the feature component i in input vector \mathbf{x} , and x_i^+ and x_i^- are the new agonist-antagonist representations receptively of feature component i . The constants x_{iMAX} and x_{iMIN} are the maximum and minimum values, respectively, for the i^{th} feature component.

Appendix II - Euclidean distance calculations.

The Euclidean distance d between the output vector and the prototype population vector p is calculated by

$$(3) \quad d = \sqrt{\sum_k \frac{(x_k - x_k^p)^2}{(x_{kMAX} - x_{kMIN})^2}},$$

where x_k is the k component of the input vector \mathbf{x} and x_k^p is the k^{th} component of the prototype population vector p . x_{kMAX} and x_{kMIN} are the maximum and minimum values, respectively, for the k^{th} feature component.

Appendix III - Log-Likelihood Ratio Testing.

The log-likelihood ratio testing is used to determine the quality of fit between the psychological data and the prediction of the neural model (Wickens 1982):

$$(4) \quad \ln L = \sum_i \ln N_i! - \sum_i \sum_j \ln f_{ij}! + \sum_i \sum_j f_{ij} \cdot \ln p_{ij},$$

where N_i is the frequency with which stimulus i was presented, f_{ij} is the observed frequency with which stimulus i was identified as stimulus j , and p_{ij} is the predicted probability with which stimulus i is identified as stimulus j .